Pharmacology, Biochemistry and Behavior 234 (2024) 173689

Contents lists available at ScienceDirect

Pharmacology, Biochemistry and Behavior

journal homepage: www.elsevier.com/locate/pharmbiochembeh

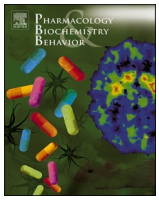

Ndufs4 KO mice: A model to study comorbid mood disorders associated with mitochondrial dysfunction

Daniël J. van Rensburg [a], Zander Lindeque [b], Brian H. Harvey [a,c,d], Stephan F. Steyn [a,*]

[a] Centre of Excellence for Pharmaceutical Sciences, Faculty of Health Sciences, North-West University, Potchefstroom, South Africa
[b] Human Metabolomics, Faculty of Natural and Agricultural Sciences, North-West University, Potchefstroom, South Africa
[c] South African Medical Research Council Unit on Risk and Resilience in Mental Disorders, Department of Psychiatry and Neuroscience Institute, University of Cape Town, South Africa
[d] The Institute for Mental and Physical Health and Clinical Translation, School of Medicine, Deakin University, Geelong, Australia

ARTICLE INFO

Keywords:
Monoamines
Mood
Oxidative stress
Tryptophan metabolism

ABSTRACT

The *Ndufs4* knockout (KO) mouse is a validated and robust preclinical model of mitochondrial diseases (specifically Leigh syndrome), that displays a narrow window of relative phenotypical normality, despite its inherent mitochondrial complex I dysfunction and severe phenotype. Preclinical observations related to psychiatric comorbidities that arise in patients with mitochondrial diseases and indeed in Leigh syndrome are, however, yet to be investigated in this model. Strengthening this narrative is the fact that major depression and bipolar disorder are known to present with deficits in mitochondrial function. We therefore screened the behavioural profile of male and female *Ndufs4* KO mice (relative to heterozygous; HET and wildtype; WT mice) between postnatal days 28 and 35 for locomotor, depressive- and anxiety-like alterations and linked it with selected brain biomarkers, viz. serotonin, kynurenine, and redox status in brain areas relevant to psychiatric pathologies (i.e., prefrontal cortex, hippocampus, and striatum). The *Ndufs4* KO mice initially displayed depressive-like behaviour in the tail suspension test on PND31 but not on PND35 in the forced swim test. In the mirror box test, increased risk resilience was observed. Serotonin levels of KO mice, compared to HET controls, were increased on PND36, together with increased tryptophan to serotonin and kynurenine turnover. Kynurenine to kynurenic acid turnover was however decreased, while reduced versus oxidized glutathione ratio (GSH/GSSG) was increased. When considering the comorbid psychiatric traits of patients with mitochondrial disorders, this work elaborates on the neuropsychiatric profile of the *Ndufs* KO mouse. Secondly, despite locomotor differences, *Ndufs4* KO mice present with a behavioural profile not unlike rodent models of bipolar disorder, namely variable mood states and risk-taking behaviour. The model may elucidate the bio-energetic mechanisms underlying mood disorders, especially in the presence of mitochondrial disease. Studies are however required to further validate the model's translational relevance.

1.1. Introduction

The *Ndufs4*$^{-/-}$ (knockout; KO) mouse lacks the *NDUFS4* (NADH: ubiquinone oxidoreductase core subunit S4) mitochondrial subunit protein that is essential for the formation and function of mitochondrial complex I (Vogel et al., 2007; Zhao et al., 2019). Ablation of complex I adversely influences mitochondrial function and leads to detrimental downstream effects, such as increased neuroinflammation and oxidative stress (Liu et al., 2015). The *Ndufs4* KO mouse is mostly used to study Leigh syndrome, a hereditary mitochondrial disease in young children (Van De Wal et al., 2022), characterized by symptoms such as psychomotor arrest or regression, retarded growth, developmental delay, muscular hypotonia or dystonia, seizures, visual defects, cardiomyopathy, respiratory failure, and overall failure to thrive (Kruse et al., 2008). Similar to the clinical setting (Stenton et al., 2022), *Ndufs4* KO mice also have a shortened life span (~50 days), compared to control animals

Abbreviations: EPM, elevated plus maze; FST, forced swim test; GSH, reduced glutathione; GSSG, glutathione disulfide; HET, heterozygous; KO, knockout; MBT, mirror box test; NAD, nicotinamide adenine dinucleotide; NWU, North-West University; OFT, open field test; PND, postnatal day; TST, tail suspension test; WT, wildtype.

* Corresponding author.
E-mail address: Stephan.steyn@nwu.ac.za (S.F. Steyn).

https://doi.org/10.1016/j.pbb.2023.173689
Received 28 August 2023; Received in revised form 3 December 2023; Accepted 4 December 2023
Available online 7 December 2023

(Kruse et al., 2008). Until postnatal day 30 (PND30), *Ndufs4* KO mice present with lowered body weight and core temperatures and decreased complex I activity (Calvaruso et al., 2012), despite having comparable muscle oxygen consumption and respiration rates (Breuer et al., 2012). From PND35, severe impairment in gait, together with decreased water and food intake, and progressive ataxia are observed (Van De Wal et al., 2022). However, the suitability of the *Ndufs4* KO mouse as a potential model to study mitochondrial dysfunction of relevance in psychiatric disorders, or the comorbid presentation of psychiatric disorders in mitochondrial diseases, have not yet been scrutinized. Interestingly, *Ndufs4* KO mice present with a brief period between PND28 and 35, where little to no deleterious bio-behavioural deficits are evident (Kruse et al., 2008). This may represent a window wherein the role of sub-clinical mitochondrial dysfunction could be explored in terms of neuropsychiatric disorders.

The understanding of mitochondrial dysfunction and its suspected role within psychiatric diseases have gained interest in recent years. Mitochondrial dysfunction can adversely influence neuronal function through direct and indirect pathways i.e., suboptimal energy production, altered kynurenine metabolism, redox stress, altered nitric-oxide synthase activity, increased apoptosis, and/or altered pyrimidine biosynthesis, fatty acid metabolism, calcium homeostasis and/or inflammation (Bustamante et al., 2007; Chen et al., 2007; Grace et al., 2006; Missiroli et al., 2020; Murphy, 2018; Wajner and Amaral, 2016; Wallace, 2007). The first sign, and arguably the largest body of evidence for the involvement of the mitochondria within these pathologies, are increases in oxidative stress markers observed in psychiatric pathologies (Salim, 2014; Smaga et al., 2015). Mitochondria regulate the glutathione antioxidant defence system (Bjørklund et al., 2021) responsible for decreasing hydroxyl radicals, peroxynitrite, superoxide radicals and other reactive oxygen species, and which are increased during mitochondrial dysfunction.

Concerning mood disorders, mitochondrial dysfunction has been linked with dysregulated synaptic strength and cellular resilience in neural circuits, resulting in altered cognition and behaviour (Manji et al., 2012), as well as increased neuroinflammation and apoptotic cascades (Allen et al., 2018; Sharma and Akundi, 2019). Clinically, patients with genetic mitochondrial disorders, such as mitochondrial epilepsy, encephalomyopathy (Fattal et al., 2007) and even neurodegenerative diseases such as multiple sclerosis (Boeschoten et al., 2017; Patten et al., 2017; Solaro et al., 2018), have a higher incidence of depression and other psychiatric disorders, when compared to the general population (Morava et al., 2010; Rezin et al., 2009). That stress is strongly associated with the pathophysiology of psychiatric diseases, such as major depressive disorder (Bleys et al., 2018; LeMoult et al., 2020), and adversely affect mitochondrial function, underlines the involvement of mitochondrial dysfunction in the etiopathology of depression. Chronic stress for instance, negatively affects electron transport chain functions, which is normalized by fluoxetine (Wen et al., 2014).

Rodent models are widely used to investigate mechanisms suspected to be involved in various psychopathologies. Some of the most popular models of anxiety, bipolar disorder, depression, and schizophrenia include the Flinders sensitive line rat (Chen et al., 2013), post-weaning social isolation rearing (Mncube and Harvey, 2022), stress-induced (Seewoo et al., 2020; Soares-Cunha et al., 2018; Wang et al., 2020), lipopolysaccharide-induced (Swanepoel et al., 2018; Wang et al., 2019) and olfactory bulbectomy (Avetisyan et al., 2016) models, which have been associated with mitochondrial dysfunction. Yet, these deficits are considered secondary constructs of the specific model. Pharmacologically induced mitochondrial dysfunction via rotenone (Santiago et al., 2010; Varga et al., 2021) and/or MPTP (1-methyl-4-phenyl-1,2,3,6-tetrahydropyridine) (Gorton et al., 2010; Santiago et al., 2010) induce decreased dopamine and serotonin levels with neuronal degradation, increased oxidative stress and altered calcium signalling (Balakrishnan et al., 2021; Gorton et al., 2010; Hu et al., 2016; Pan-Montojo et al., 2010; Przedborski et al., 2000; Santiago et al., 2010; Swathi et al., 2013; von Wrangel et al., 2015), as well as behavioural profiles akin to schizophrenia (Varga et al., 2021), bipolar disorder (Damri et al., 2021), and major depressive disorder (Okano et al., 2019; Sharma and Akundi, 2019). These behavioural changes are also attenuated by haloperidol (Varga et al., 2021), lithium (Damri et al., 2021), venlafaxine (Sharma et al., 2016), sertraline (Sharma et al., 2016), selegiline (Okano et al., 2019), and pramipexole (Okano et al., 2019), further strengthening an argument for deficient bio-energetic systems in these psychopathologies.

Considered together, animal models that have mitochondrial dysfunction as an underlying construct may shed light on the role of dysfunctional bio-energetic systems in the aetiology of mood disorders or the co-presentation thereof in mitochondrial diseases [48]. It is worth noting that the *Ndufs4* mice are generally used for neurodegenerative and mitochondrial disease research and could therefore provide the link between mitochondrial dysfunction and mood disorders within the same construct (van Rensburg et al., 2022).

The current study therefore explored the neuropsychiatric bio-behavioural profile of the *Ndufs4* KO mouse and compared it to the *Ndufs4*$^{+/+}$ (wildtype; WT) and heterozygous (HET; *Ndufs4*$^{+/-}$) counterparts during the asymptomatic PND28–35 window. We therefore aimed to determine whether behavioural and neurochemical parameters, relevant for depression, differed across these genotypes prior to the onset of overt behavioural changes (PND 36 onwards). *Ndufs4* KO were therefore screened with behavioural tests focusing on depressive and anxiety-like constructs, while an array of neurochemical markers associated with depression and mitochondrial function were measured. We hypothesized that the *Ndufs4* KO mouse would present with increased anxiety- and depressive-like behaviour, together with decreased brain serotonin, tryptophan, and increased kynurenine and quinolinic acid synthesis. Furthermore, regional brain reduced (GSH) and oxidized (GSSG) glutathione would be dysregulated more prominently in *Ndufs4* KO mice.

1.2. Materials and methods

1.2.1. Experimental layout

Animals were divided into the different genotype cohorts, WT (n = 12), HET (n = 12) and KO (n = 11), containing an even number of males and females. As summarized in Fig. 1, behavioural testing started on PND28 and continued until PND35. Because genotyping could only be performed on PND21, behavioural testing was only introduced following a recovery and habituation time following genotyping (see below). Behavioural screening tests, for general locomotor activity (open field tests (PND28–30)), depressive-like behaviour (tail suspension (PND31) and forced swim tests (PND35)), and anxiety-like/risk resilience behaviour (elevated plus maze (PND33) and mirror box test (PND34)) were included. The tests were performed form least to most stressful and performed before the onset of the mentioned detrimental behavioural deficits. On PND36, animals were euthanized by decapitation, whereafter brain areas (hippocampus, prefrontal cortex, and striatum) were removed and stored at −80 °C for neurochemical analyses. Due to a malfunction during neurochemical analysis, some samples of each cohort were lost and consequently decreased the group sizes (groups sizes are indicated in the respective figures as individual data points).

1.2.2. Animals and housing

Male and female mice (aged 21 days at the onset of the experimentation) were randomly selected from the housing colony at the DSI/NWU Vivarium (SAVC reg. no. FR15/13458; AALAC accreditation international file #1717) of the NWU, RSA. Before experimentation commenced, all animals were group-housed in same sex cages [35 (l) ×

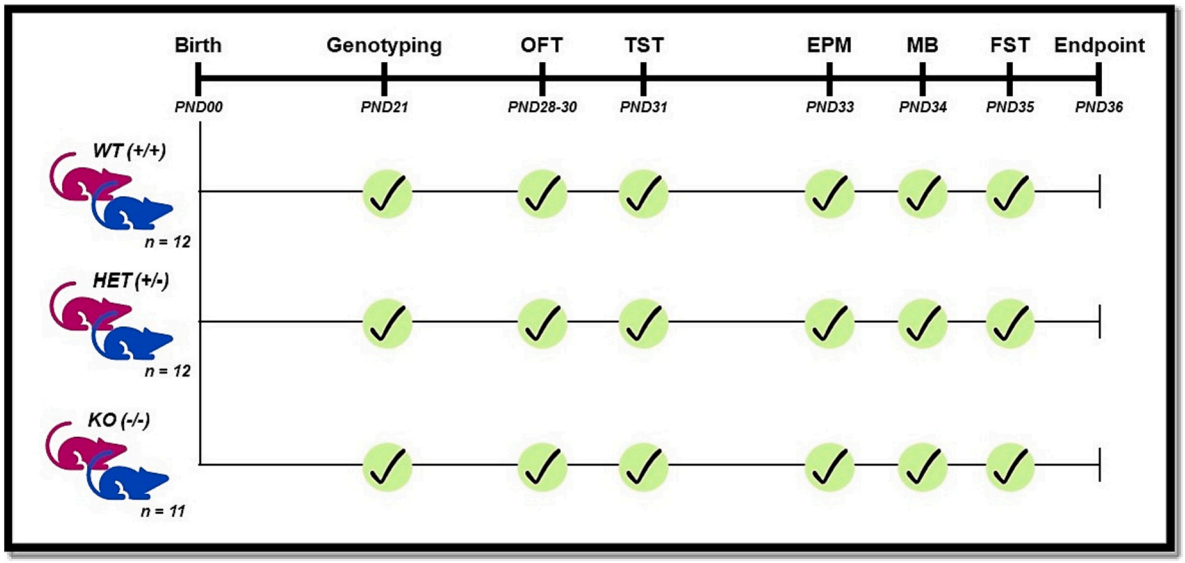

Fig. 1. Study layout summary.
Male and female Ndufs4 mice were genotyped on PND21, whereafter their bio-behavioural profiles were screened between PND28 and 36 to determine their suitability for neuropsychiatric research. EPM: elevated plus maze; FST: forced swim test; HET: heterozygous; KO: knockout; MB: mirror box test; OFT: open field test; PND: postnatal day; TST: tail suspension test; WT: wild type.

20 (*w*) × 13 (*h*) cm; Techniplast® S.P.A., Varese, ITA; four to six animals per cage]. Cages were automatically climate-controlled at a temperature of 23 °C and a relative humidity of 50 %, with paper towel and a small white polyvinyl chloride pipe [10 (*l*); 4 (Ø) cm] as environmental enrichment. A normal 12-h light/dark cycle (lights on at 06:00, off at 18:00) was used, with food and water provided ad libitum throughout the investigation period. The animal's weight and food intake were measured daily during the light cycle. Cages were cleaned, and fresh corncob supplied weekly between 08:00 and 10:00.

1.2.3. Genotyping

As previously described by Terburgh et al. (2019), DNA was isolated according to manufacturer instructions using the Zymo Research Quick-DNA™ Miniprep Plus kit (Inqaba Biotec, #D4068). The isolated DNA was quantified using a NanoDrop One Microvolume UV–Vis spectrometer (Thermo Fisher Scientific). A PCR reaction was performed to confirm deletion of exon 2 of *NDUFS4* using specific forward (5′-AGCCTGTTCTCATACCTCGG-3′) and reverse (5′-TTGTGCTTACAGGTTCAAAGTGA-3′) primers (0.5 μM each) designed for the *NDUFS4* gene, along with 1× Phire Tissue Direct PCR Mastermix (Thermo Fisher Scientific, #F-170L), nuclease-free water and 25 ng DNA. Thermal cycling conditions consisted of an activation step at 98 °C for 5 min followed by 34 cycles of 98 °C for 5 s, 57.3 °C for 5 s and 72 °C for 20 s, with final isothermal step at 72 °C for 1 min. When analysing the DNA fragments, a 1229 bp band, indicated a WT ($Ndufs4^{+/+}$), a 429 bp band a homozygote ($Ndufs4^{-/-}$; KO), and the presence of both bands indicated a HET ($Ndufs4^{+/-}$). From in-house experience, a yield of 25 % (KO), 50 % (HET) and 25 % (WT) could be expected.

1.2.4. Behavioural testing

Behavioural testing was performed between PND28 and 35 and included the open field and tail suspension tests (PND28 to 31), elevated plus maze (PND33), mirror box test (PND34) and forced swim test (PND35) during the dark cycle (i.e., after 19:00) of the animals. Repeating the same test (for depressive-like behaviour) was avoided to ensure that the mice did not habituate during the first test and impact consequent analyses. Moreover, because of the uncertainty of whether the KO mice would be able to take part in (and survive) the forced swim test, largely because of their documented decline in locomotor activity, this test was only performed towards the end of the study. Behaviour was analysed by automated software (Ethovision XT14; Noldus Information Technology BV, Wageningen, NLD). For the manually scored behavioural tests (tail suspension and forced swim), the analysing researcher was blinded to the experimental groups to minimize research bias, with behavioural scoring done with a continuous timer (FST Scoreboard 2.0 software, NWU, RSA) (Steyn et al., 2020).

1.2.5. Open field test

The open field test is typically conducted to measure inherent locomotor ability preceding the forced swim test. In the case of the *Ndufs4* mouse model, special consideration was afforded to locomotor ability, as significant decreases in the gait analyses of the genotype have previously been reported (Van De Wal et al., 2022). Such decreased locomotion could confound test outcomes, specifically in the forced swim test. Consequently, the open field test was performed over three consecutive days (PND28 to 30) to determine baseline locomotor activity and whether this would show an accelerated or more pronounced decline in KO animals compared that of mice in the HET and WT groups. As previously described (Seibenhener and Wooten, 2015), mice were placed in the centre of a 0.5 m^2 black opaque arena and left to freely explore for 10 min, under dim red light. Total distance travelled was measured and interpreted as indication of general locomotor activity.

1.2.6. Tail suspension test

The tail suspension test is used to measure depressive-like behaviour (Cryan et al., 2005), and was performed according to previous reports (Castagné et al., 2011; Cryan et al., 2005) on PND31 in a custom made testing arena [50 (*l*) × 15 (*w*) × 30 (*h*) cm]. Briefly, on the day of testing, mice were suspended by their tails with adhesive tape, applied three-quarters of the distance from the base of the tail, from a suspension hook for 6 min under red light. To avoid injury, the suspension hook was forced through the adhesive tape as close as possible to the tail to ensure the animal hung with its tail in a straight line (Castagné et al., 2011). Behaviour was recorded with a camera mounted in front of the behavioural test, with the total time spent immobile recorded and interpreted as an indication of depressive-like behaviour.

1.2.7. Elevated plus maze

The elevated plus maze is a validated model used to measure anxiety-like behaviour in rodents and consists of a black Plexiglas® plus shaped maze, with the platform elevated approximately 50 cm above the floor with two closed [35 (*l*) × 20 (*w*) × 10 (*h*) cm] and two open arms [35 (*l*) × 20 (*w*) cm]. To prevent animals from falling off, a 1 cm transparent Plexiglas® border is fixed along the borders of the open arms. On PND33, mice were placed in the centre of the maze, facing the open arm opposite the investigator, and allowed to freely explore for 5 min under red light (Regenass et al., 2018). Increased time spent in the closed arms is considered indicative of anxiety-like behaviour. In all instances, entrance into an arm was recorded when the centre point, as defined by the automated scoring program, entered the specific arm. The total distance moved was also used as a co-variant when analysing the forced swim test.

1.2.8. Mirror box test

The mirror box test is used to measure anxiety-like behaviour. The test was performed on PND34 under dim red light in a square Plexiglas® box [50 (*l*) × 50 (*w*) × 30 (*h*) cm] with an enclosed, dark chamber [17 (*l*) × 17 (*w*) × 30 (*h*) cm] in one corner (Wolmarans et al., 2022). A 25 cm^2 opening in the dark chamber allowed free and voluntary access to the larger arena, that consisted of a white Plexiglas® floor and mirrored walls to evoke anxiety and bolster the aversive character of the area. White floors and mirrors exacerbate the aversive nature of an open field arena (Carola et al., 2002; Crawley and Goodwin, 1980; Pich and Samanin, 1989; Smythe et al., 1996) and induce avoidance behaviour in mice (Fuss et al., 2013; Kliethermes et al., 2003; Reddy et al., 2011; Walf et al., 2009). On PND34, mice were placed on the dark-floored compartment of the open field and left to freely explore for 6 min. Digital video cameras above all arenas recorded behaviour with time spent in the mirrored and closed areas of the arena scored by the automated software.

1.2.9. Forced swim test

The forced swim test is widely-used screening test for depressive-like behaviour (Cryan et al., 2002). On PND35, animals were placed in an inescapable Perspex® cylinder (50 (*h*); 15 (⌀) cm), filled with water at a temperature of 25 ± 1 °C for 6 min, with only the last 5 min used for analysis – similar to the methodology of Emmerzaal et al. (2020b). Behaviour was recorded by a camera mounted in front of the test arena. Time spent immobile (floating with no active movement or passive leg twitching except those movements necessary to keep the mouse's head above water) was considered an indication of depressive-like behaviour. Following the test, mice were dried using paper towel and returned to their cages.

1.2.10. Tissue collection, storage, and analysis

On PND36, animals were euthanized via decapitation, according to approved procedures. Brain regions (hippocampus, prefrontal cortex, and striatum) were harvested and stored at −80 °C. Brain areas were snap-frozen in liquid nitrogen and stored at −80 °C. Each brain tissue sample was individually weighed prior to preparation. Hereafter, 250 μl of the internal standard solution, ethyl 4-hydroxy-2-quinolinecarboxylate (EHQC), with a concentration of 100 μg/ml using a solvent mix of 0.1 % formic acid in 100 % MeOH, was added to each brain sample. The mixtures were homogenized by sonication (twice for 12 s, at an amplitude of 14 μ; MSE ultrasonic disintegrator, Nuaillé, FRA); this is the preferred method to ensure cell rupture for small sample and homogenate volume sizes (Keller et al., 1976). The mixture was left on ice for 20 min to complete protein precipitation and centrifuged at 20817 *g* for 20 min at 4 °C. The supernatant was transferred to a HPLC sample vail. The analytical HPLC column used was a Venusil ASB C18 column (2.1 × 150 mm, particle size 3 μm, purchased from Agela Technologies, Torrance, CA, USA). The Ultivo Triple Quadrupole LC/MS System, controlled by the MassHunter software from© Agilent Technologies, Inc. (Santa Clara, CA 95051 US) was used. A gradient mobile phase consisting of A: 0.1 % formic acid/HPLC grade water and B: 0.1 % formic acid/methanol was prepared. The MassHunter software program was then programmed to inject 1 μl of the prepared sample onto the LC-MS system for analysis.

1.2.11. Power and statistical analyses

Statistical analyses were performed in IBM® SPSS® Statistics (version 28) and Graphpad Prism® (version 10), assisted by Laerd Statistics® (https://statistics.laerd.com). The initial power analysis was performed in G*Power® (version 3.1; Universität Kiel, GER). Briefly, an A priori test (*ANCOVA: Fixed effects, omnibus, one-way*), set at an effect size of 0.4, 0.05 α error probability, and 0.8 power, suggested 18 animals per group. However, in line with literature (Emmerzaal et al., 2020a; Emmerzaal et al., 2020b; Lindeque et al., 2018; Miller et al., 2021) a consequent sensitivity analysis supported twelve animals per group.

All data sets were screened for outliers (Grubbs' test with $\alpha = 0.05$ accepted as significant) and tested for normality of distribution with the Shapiro-Wilk test. Identified outliers were reported in the legend of each data set. Of note, sex was not hypothesized to play a significant role in the outcome of the measured parameters, due to the juvenile age of the mice. Still, data sets are presented as individual data points, representing both sexes, and were visually inspected for obvious sexual differences. Regardless, appropriate statistical analyses that consider sex as an influential factor, are available as Supplementary data.

Consequently, a one-way Welch (with Dunnett's T3 post-hoc test) ANOVA (analysis of variances) was used to analyse group differences between genotypes, whereas a Kruskal-Wallis *H*-test (with Dunn's post-hoc test) was performed in instances where the assumption for normality of distribution was not true (indicated as X^2). To control for the influence of locomotor activity on behaviour (i.e., in the case of the tail suspension and forced swim tests), a one-way ANCOVA (analysis of covariance) was performed with average distance moved used as the co-variant for time spent immobile. In all instances, significance was accepted as $p < 0.05$. Finally, all statistical analyses were followed up with effect magnitude calculations (Cumming, 2014; Lakens, 2013) that strengthen reported statistical differences (Cohen, 2013). The eta (η^2) and partial eta squared (η_p^2), and unbiased Cohen's *d* (d_{unb}) values were used to quantify the effect magnitude of overall and intergroup differences, respectively (Du Sert et al., 2020). Large effect sizes were accepted as $\eta^2 \geq 0.14$ (Ellis, 2010) and $d_{unb} \geq 0.8$ (Sullivan and Feinn, 2012). All effect magnitude calculations were performed in Exploratory Software for Confidence Intervals (Cumming, 2014).

1.3. Results

1.3.1. Body weight

Although the regression lines of the weight gain rate (Fig. 2A) deviated significantly from a zero slope ($p \leq 0.0005$) for all three genotypes, there were no statistically significant differences between these three slopes ($F_{2,\ 506} = 0.48$, $p = 0.62$). Still, the KO cohort, on average weighed less than the HET and WT genotypes, evident by the difference in elevation of the regression lines ($F_{2,\ 508} = 204$, $p \leq 0.0005$) and continuous lower mean values.

1.3.2. Open field test

As summarized in Table 1, there were statistical differences between the genotype groups ($F_{2,\ 20.6} = 5.24$, $p = 0.01$; $\eta^2 = 0.2$ [0.1; 0.4]) in Trial 1, with the KO animals covering less distance than both the HET ($p = 0.03$; $d_{unb} = 1.1$ [0.3; 2.1]) and WT animals ($p = 0.03$; $d_{unb} = 1.1$ [0.3;

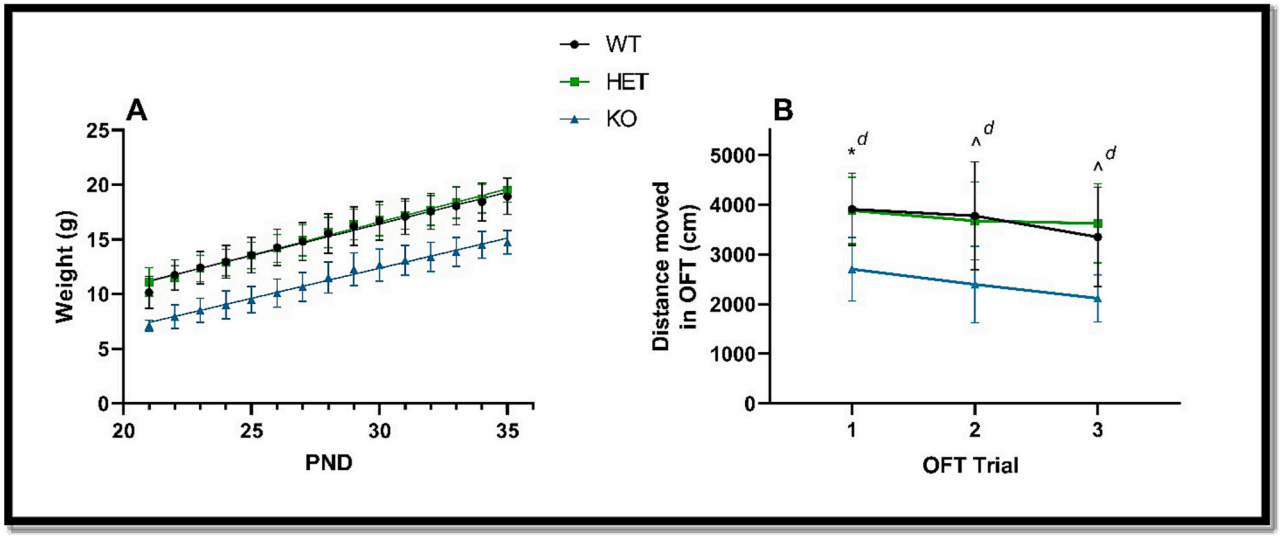

Fig. 2. Weight gained over the investigational period and locomotor activity over consecutive open field tests.
Daily weight gain (A) between PND21 and 35 (KO[a]), as well as the mean distance moved (B) over three consecutive open field test trials (WT[b] | KO[a]). Data points represent the mean ± SEM (A) and 95 % CI (B). Statistical details are reported in the text, with * indicating statistical differences between KO and both HET and WT, whereas ^ highlights differences between KO and HET. [a)] <12 animals due to lower-than-expected birth-rates at the requested date. [b)] Outlier identified in the first trial and removed due to it not representing the target population.

Table 1
Distance moved over the three open field test trials.
Trial 1 was conducted on PND28, Trial 2 on PND29, and Trial 3 on PND30. The mean distance moved over all three trials was used as a co-variant in the analyses of the tail suspension test. Statistical details are reported in the text.

Open field test	Distance moved by different genotypes *mean* ± *SD* (*n*)			Sig. (*KO* vs)
	WT	HET	KO	
Trial 1 (PND28)	3907.99 ± 1079.12 cm (*11*[a])	3881.26 ± 1048.46 cm (*12*)	2703.16 ± 949.15 cm (*11*)	HET WT
Trial 2 (PND29)	3775.98 ± 1613.50 cm (*11*[a])	3674.16 ± 1232.09 cm (*12*)	2393.14 ± 1143.88 cm (*11*)	HET
Trial 3 (PND30)	3349.98 ± 1489.61 cm (*11*[a])	3622.56 ± 1256.25 cm (*12*)	2114.94 ± 661.22 cm (*10*)	HET
Mean	3677.11 ± 1225.81 cm (*11*[a])	3725.99 ± 1066.15 cm (*12*)	2251.29 ± 633.91 cm (*10*)	HET WT

[a] Outlier identified and removed.

2.1]). In Trial 2 ($F_{2,\ 20.1} = 4.18$, $p = 0.03$; $\eta^2 = 0.2$ [0.0; 0.4]), KO mice only differed from HET mice ($p = 0.05$; $d_{unb} = 1.0$ [0.2; 2.0]). Similarly, in Trial 3 ($F_{2,\ 18.5} = 7.78$, $p = 0.004$; $\eta^2 = 0.2$ [0.01; 0.4]), KO animals covered less distance only in relation to HET ($p = 0.01$; $d_{unb} = 1.4$ [0.5; 2.4]).

In Fig. 2B, despite the slope of the regression line (*not shown*) of the KO group deviating significantly from zero ($F_{1,\ 1} = 1025$, $p = 0.02$), the slopes of all three regression lines were comparable ($F_{2,\ 3} = 2.68$, $p = 0.22$); allowing for a pooled regression line (irrespective of genotype) to be calculated ($y = -217\times + 3726$). Moreover, when comparing the mean distance moved across all three trials (Table 1), significant differences were observed ($F_{2,\ 18.9} = 10.3$, $p < 0.001$; $\eta^2 = 0.3$ [0.04; 0.5]), with KO animals covering less distance compared to both HET ($p = 0.002$; $d_{unb} = 1.1$ [0.3; 2.1]) and WT ($p = 0.02$; $d_{unb} = 1.0$ [0.1; 1.9]) animals. This parameter was consequently used as a co-variant to analyse the tail suspension test (see below).

1.3.3. Tail suspension test

On PND31, there were statistical differences between genotypes for time spent immobile in the tail suspension test (Fig. 3A and Table 2), after controlling for distance moved in the open field test ($F_{2,\ 29} = 6.84$, $p = 0.004$; $\eta_p^2 = 0.3$). *Ndufs4* KO mice were more immobile than WT controls ($p = 0.003$). The mean distance moved in the open field test, significantly influenced time spent immobile in the tail suspension test ($F_{1,\ 29} = 14.72$, $p < 0.001$; $\eta_p^2 = 0.3$).

1.3.4. Forced swim test

On PND35, the mean distance moved in the elevated plus maze, had no significant effect on time spent immobile in the forced swim test (Fig. 3B and Table 2; $F_{1,\ 29} = 0.28$, $p = 0.60$; $\eta_p^2 = 0.01$). The distance moved of the elevated plus maze was used, rather than that of the open filed test, to control for locomotor deficits more accurately closer to the time of analyses. There was however no statistically significant difference when correcting this parameter with the distance moved in the open field test (*Supplementary data*). Regardless, after controlling for this, there were no statistical differences between genotypes for time spent immobile in the forced swim test ($F_{2,\ 29} = 0.77$, $p = 0.47$; $\eta_p^2 = 0.5$).

1.3.5. Mirror box test

In Fig. 4A, there were statistically significant differences between genotypes for average duration per exploration bout in the mirror box test ($F_{2,\ 18.5} = 5.93$, $p = 0.01$; $\eta^2 = 0.3$ [0.07; 0.5]), with KO mice spending more time in the mirrored area per bout, compared only to HET ($p = 0.02$; $d_{unb} = 1.4$ [0.5; 2.4]) counterparts.

1.3.6. Elevated plus maze

In Fig. 4B, no statistical differences existed between genotypes for time spent in the open arms of the maze ($X^2_{(2)} = 2.68$, $p = 0.26$; $\eta^2 = 0.1$ [0.0; 0.2]). As for total distance moved (Fig. 4C), there were statistical differences between the genotypes ($F_{2,\ 20.0} = 4.52$, $p = 0.02$; $\eta^2 = 0.2$ [0.0; 0.3]), with KO animals only covering less distance than their HET counterparts ($p = 0.02$; $d_{unb} = 1.2$ [0.3; 2.2]). As before, this data was used as co-variant in the forced swim test analysis (Fig. 3B).

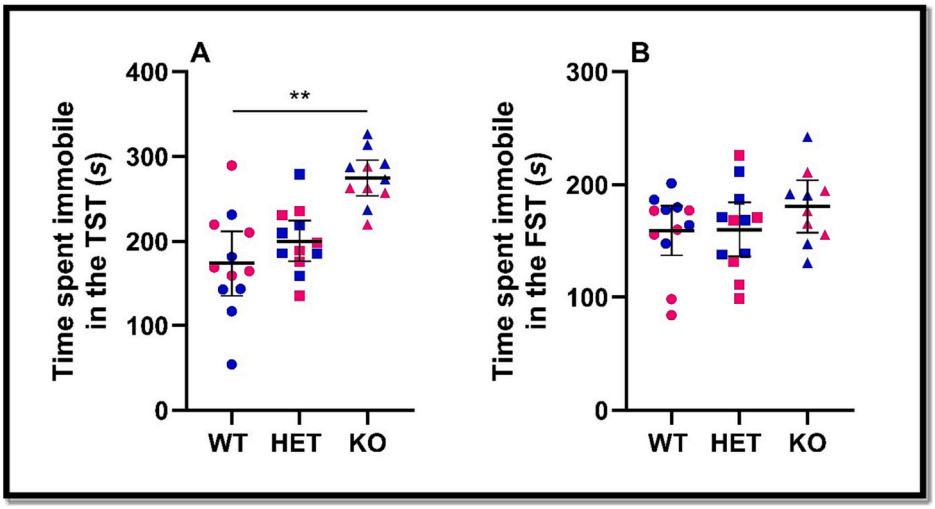

Fig. 3. Time spent immobile in the tail suspension and forced swim tests.
The tail suspension test (A) as performed on PND31 (KO[a]) and the forced swim test (B) as performed on PND35 (KO[a, b]). Male and female mice are presented as blue and red points, respectively. Data represents the unadjusted mean ± 95 % CI, with statistical details reported in the text, and ** $p \leq 0.01$ vs. indicated group. [a)] Due to lower-than-expected birth-rates in the given time, <12 animals were obtained. [b)] Animal excluded due to behavioural test malfunction.

Table 2
Original and adjusted immobility times in the TST and FST.
Values adjusted with mean distance moved in the OFT (for TST) and EPM (for FST). The TST was conducted on PND31 and the FST on PND35. Although the values presented in the figures are the unadjusted values, the adjusted values are presented here to inform the reader of the significance of the co-variant effect. Statistical details are reported in the text.

Time spent immobile in tail suspension and forced swim tests				
Genotypes	Tail suspension test (*s*)		Forced swim test (*s*)	
	Unadjusted (± SD)	Adjusted (± SEM)	Unadjusted (± SD)	Adjusted (± SEM)
WT	174.20 ± 63.24	184.62 ± 11.72	159.34 ± 35.03	159.90 ± 10.59
HET	200.17 ± 38.15	211.80 ± 11.33	159.57 ± 39.93	160.84 ± 11.27
KO	280.16 ± 26.94	254.75 ± 13.67	180.84 ± 32.62	178.78 ± 12.19

1.3.7. Oxidative stress markers

In Fig. 5, there were statistical differences between genotypes for striatal (Fig. 5A; $F_{2,11.0} = 23.58$, $p < 0.001$; $\eta^2 = 0.6$ [0.3; 0.8]) and hippocampal (Fig. 5B; $F_{2,\ 11.7} = 101.66$, $p < 0.001$; $\eta^2 = 0.6$ [0.3; 0.8]), but not for cortical (Table 3; $F_{2,\ 14.6} = 0.41$, $p = 0.67$; $\eta^2 = 0.4$ [0.0; 0.2]) GSH/GSSG values. KO mice had higher striatal ($p < 0.001$, $d_{unb} = 3.1$ [1.8; 4.6]) and hippocampal ($p < 0.001$, $d_{unb} = 6.5$ [4.4; 9.2]) values, compared to HET counterparts. Relative to WT controls, only KO striatal GSH/GSSG values were higher ($p = 0.02$, $d_{unb} = 1.4$ [0.4; 2.5]). All individual values used to calculate the ratios are available as supplementary data.

1.3.8. Serotonin

There were statistically significant differences between genotypes for hippocampal (Fig. 6A; $F_{2,\ 10.8} = 9.60$, $p = 0.004$; $\eta^2 = 0.5$ [0.2; 0.7]) and cortical (Fig. 6B; $F_{2,\ 14.2} = 5.53$, $p = 0.02$; $\eta^2 = 0.4$ [0.1; 0.6]), but not

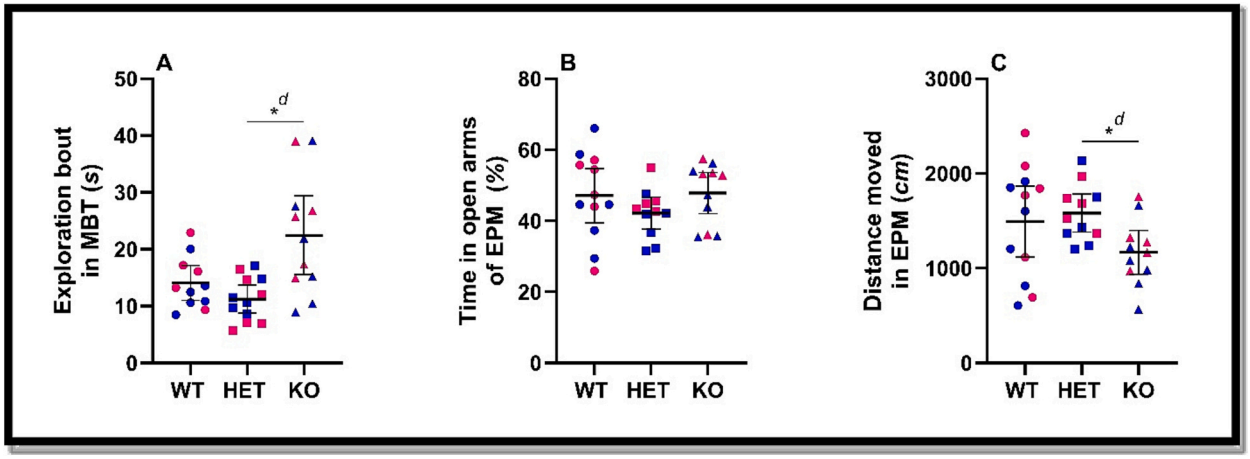

Fig. 4. Time spent in the open area of the mirror box, and open arms of the elevated plus maze, together with distance moved.
The mirror box test was performed on PND34, with time spent/bout in the mirrored area of the mirror box (A) measured (WT[a] | KO[b]). The elevated plus maze test was performed on PND33, with percentage time spent in open arms (B) and distance moved (C) measured (HET[c] | KO[b]). Male and female mice are presented as blue and red points, respectively. Data represents the mean ± 95 % CI, with statistical details reported in the text, and * $p < 0.05$ and d ≥ 0.8 (large effect) vs. indicated group. [a)] Outlier identified and removed. [b)] <12 animals due to lower-than-expected birth-rates in the given time. [c)] Animal excluded due to behavioural test malfunction.

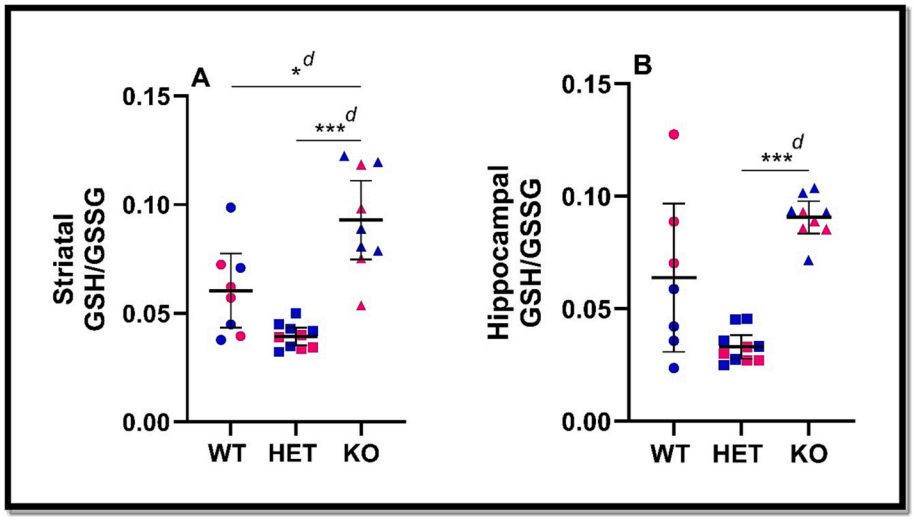

Fig. 5. Striatal and hippocampal GSH/GSSG ratios.
The GSH/GSSG ratios measured in the striatum (A) and hippocampus (B) were calculated as (GSG + 2(GSSG))/((2 * GSSG)100) (Benzi and Moretti, 1995), and are indicative of the redox state. Male and female mice are presented as blue and red points, respectively. Data represents the mean ± 95 % CI, with statistical details reported in the text, and *** p < 0.001 and d ≥ 0.8 (large effect) vs. indicated group.

striatal (Table 3; $F_{2,\ 14.0} = 3.40$, $p = 0.06$; $\eta^2 = 0.3$ [0.2; 0.5]) serotonin. KO mice had higher hippocampal ($p = 0.01$, $d_{unb} = 3.1$ [1.0; 3.4]) and cortical ($p = 0.04$, $d_{unb} = 1.4$ [0.4; 2.5]) serotonin concentrations, compared to HET genotypes.

1.3.9. Tryptophan metabolism

There were statistical differences between genotypes for hippocampal (Fig. 6C; $F_{2,\ 10.9} = 7.43$, $p = 0.01$; $\eta^2 = 0.4$ [0.1; 0.6]) and cortical (Fig. 6D; $F_{2,\ 13.70} = 5.38$, $p = 0.02$; $\eta^2 = 0.3$ [0.03; 0.5]) but not for striatal (Table 3; $F_{2,\ 14.5} = 2.80$, $p = 0.09$; $\eta^2 = 0.3$ [0.0; 0.5]) serotonin/tryptophan values. KO mice had higher values than their HET counterparts in both the hippocampus ($p = 0.02$, $d_{unb} = 1.7$ [0.7; 2.8]) and prefrontal cortex ($p = 0.01$, $d_{unb} = 1.5$ [0.5; 2.6]).

In terms of the conversion of tryptophan to kynurenine, there were statistical differences between genotypes for striatal (Fig. 6E; $F_{2,\ 14.19} = 7.26$, $p = 0.01$; $\eta^2 = 0.4$ [0.04; 0.6]) and cortical (Fig. 6F; $F_{2,\ 14.61} = 12.30$, $p < 0.001$; $\eta^2 = 0.6$ [0.2; 0.7]) but not for hippocampal (Table 3; $F_{2,\ 12.6} = 2.36$, $p = 0.14$; $\eta^2 = 0.2$ [0.0; 0.4]) kynurenine/tryptophan values. KO mice had higher cortical kynurenine/tryptophan values than both HET ($p = 0.001$, $d_{unb} = 2.0$ [0.9; 3.2]) and WT ($p = 0.001$, $d_{unb} = 2.1$ [1.0; 3.5]) controls. Intriguingly, striatal levels only differed between HET and WT genotypes ($p = 0.009$, $d_{unb} = 1.3$ [0.3; 2.3]). All individual values used to calculate the ratios are available as supplementary data.

1.3.10. Kynurenine metabolism

There were statistical differences between genotypes for striatal (Fig. 7A; $F_{\ 2,\ 14.83} = 7.39$, $p = 0.006$; $\eta^2 = 0.5$ [0.1; 0.6]), hippocampal (Fig. 7B; $F_{\ 2,\ 11.84} = 8.55$, $p = 0.005$; $\eta^2 = 0.3$ [0.03; 0.5]) and cortical (Fig. 7C; $F_{\ 2,\ 15.82} = 8.75$, $p = 0.003$; $\eta^2 = 0.5$ [0.1; 0.6]) kynurenic acid/kynurenine values. Specifically, KO mice displayed lower hippocampal ($p = 0.007$, $d_{unb} = 1.6$ [0.6; 2.7]) and cortical ($p = 0.002$, $d_{unb} = 1.9$ [0.8; 3.1]) values, compared to HET animals. In the striatum, both KO ($p = 0.02$, $d_{unb} = 1.4$ [0.4; 2.4]) and WT ($p = 0.005$, $d_{unb} = 1.6$ [0.6; 2.8]) animals had lower values than their HET counterparts. All individual values used to calculate the ratios are available as supplementary data.

1.4. Discussion

Ndufs4 KO mice have reduced mitochondrial complex I function (Miller et al., 2021), which severely alters behavioural functioning especially from day 36 onwards, and ultimately limits the lifespan of the KO versus WT and HET mice (Kruse et al., 2008). Days 28 to 35 thus presents with an opportune window where mitochondrial dysfunction is present, yet without any observable and/or severe pathologies in KO mice (Kruse et al., 2008). This period may represent a pre-syndromic phase that is characterized by psychosomatic alterations, followed by neural degeneration and the onset of behavioural deficits (PND36 onwards), making it ideal to assess co-presenting neuropathology. To investigate this, male and female KO mice were subjected to a battery of behavioural tests during this pre-syndromic phase. Sex did not significantly affect the investigated parameters (see *Supplementary data*), and hence the current findings were interpreted independent of sex.

Like previous studies (Kruse et al., 2008; Miller et al., 2021), the KO mice presented with hair loss (*data not shown*) and lower body weight, compared to both HET and WT genotypes. Despite this, they showed comparable weight gain (Fig. 1A), supporting PND28–35 as a window of relative phenotypical normality. Of note, due to their comparable phenotype and metabolic profiles (Kruse et al., 2008; Van De Wal et al., 2022), KO mice are usually compared to either WT controls, or to a pooled cohort of WT and HET mice (Johnson et al., 2020). Between PND28 and 30, the *Ndufs4* KO mice displayed a general reduction in locomotor activity, relative to WT and HET mice (Fig. 2B and Table 1). Despite this difference however, the rate of change in locomotor activity over time (Fig. 1B) was similar between the three genotypes, again suggesting they retained functional ability to move at this specific age.

The *Ndufs4* KO mice did not display increased anxiety-like behaviour on PND33 (Fig. 4B) versus either WT or HET, suggesting that whole body *NDUFS4* knockout is not a primary contributor to anxiety-like behaviour. To further investigate this theme, animals were subjected to the anxiogenic mirror box test on PND34. Here, *Ndufs4* KO mice unexpectedly spent more time exploring an anxiogenic environment, compared to the HET animals (Fig. 4A), suggesting a less anxious profile as well as greater risk taking behaviour in an aversive environment (Kara and Einat, 2013). It is however important to consider that the *Ndufs4* KO mice are known to develop visual impairments (Kruse et al., 2008), which could have been a confounding factor in both the anxiety tests, and therefore warrants further investigation.

Depressive-like behaviour, using the tail suspension and forced swim tests, were performed at two different time points to determine whether a declining bio-energetic system may contribute to a worsening of

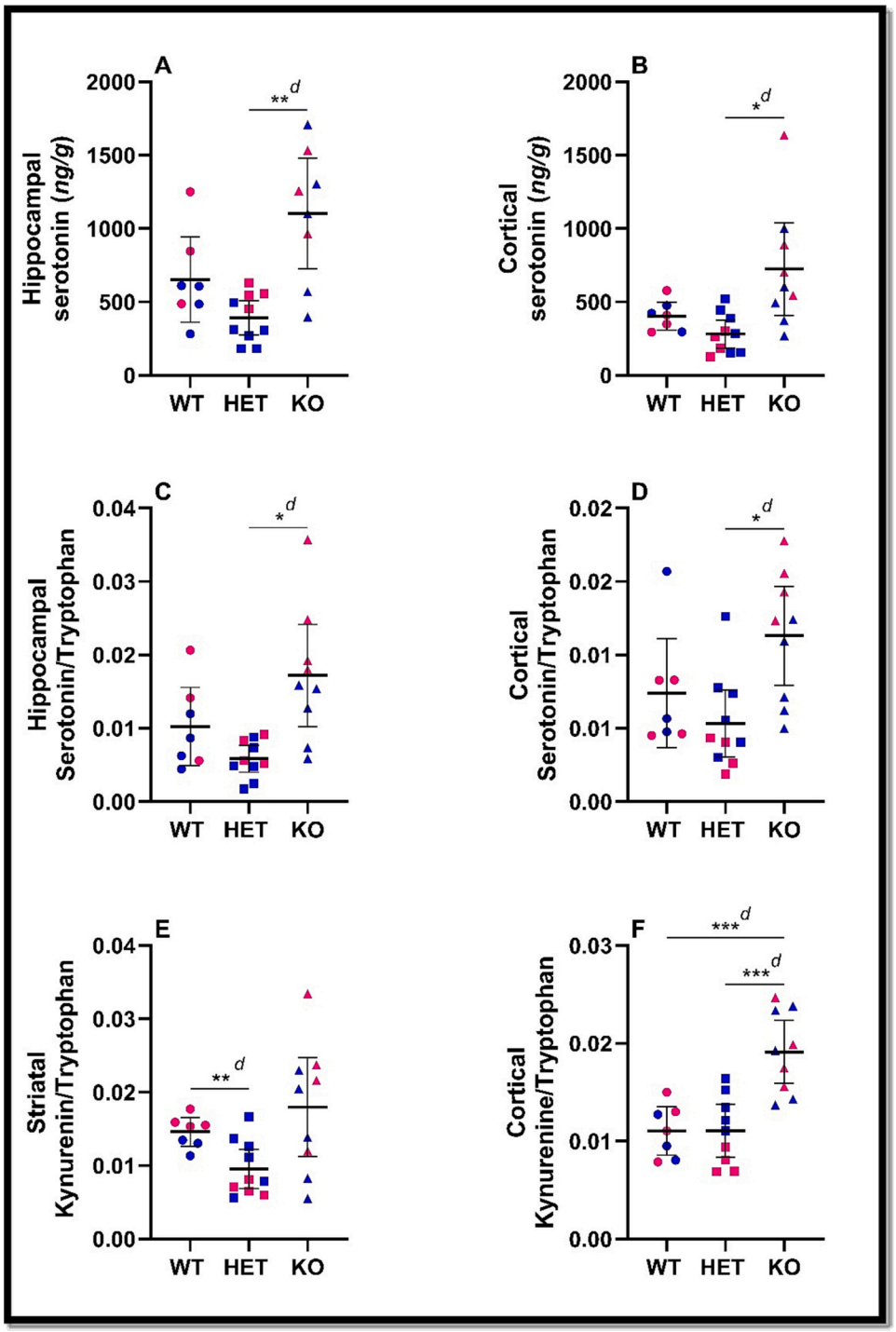

Fig. 6. Tryptophan pathway markers in different brain regions.
Serotonin measured in the (A) hippocampus and (B) frontal cortex. The serotonin/tryptophan ratios as measured in the (C) hippocampus and (D) frontal cortex (WT[a]). The kynurenine/tryptophan ratios as measured in the I striatum and (F) frontal cortex (WT[a] | HET[a]). Male and female mice are presented as blue and red points, respectively. Data represents the mean ± 95 % CI, with statistical details reported in the text, ** $p \leq 0.01$, *** $p < 0.001$, and $d \geq 0.8$ (large effect) vs. indicated group. [a)] Outlier identified and removed.

depressive-like behaviour. After correcting for the mean locomotor activity in the open field tests, the *Ndufs4* KO mice displayed significantly increased immobility (depressive-like behaviour) in the tail suspension test on PND31, compared to WT genotypes (Fig. 3A and Table 2). Therefore, at least at this apparent pre-syndromic stage, *Ndufs4* KO mice demonstrate increased depressive-like behaviour. As noted earlier, depression is also observed in patients with various mitochondrial diseases, including Leigh syndrome.

Four days later however (on PND35), *Ndufs4* KO mice (irrespective of sex) failed to display depressive-like behaviour in the forced swim test (Fig. 3B). That said, swimming behaviour was corrected with locomotor activity as displayed in the elevated plus maze, and not the open field test, due to the statistically significant decline in locomotor activity reported in the latter test (Fig. 4D). Of note, similar results were obtained when correcting with the distance moved in the open field test (see *Supplementary data*). Still, this relatively quick shift in behavioural

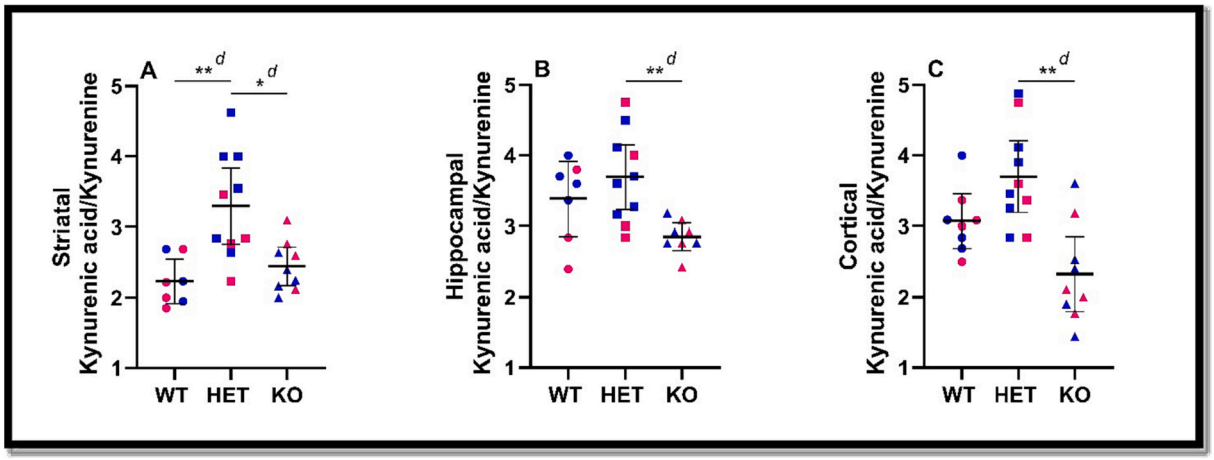

Fig. 7. Kynurenic acid/kynurenine ratio for each genotype
The serotonin/tryptophan ratios as measured in the (A) striatum (WT[a]), (B) hippocampus (KO[a]) and (C) frontal cortex. Male and female mice are presented as blue and red points, respectively. Data represents the mean ± 95 % CI, with statistical details reported in the text, * $p < 0.05$, ** $p \leq 0.01$ and $d \geq 0.8$ (large effect) vs. indicated group.

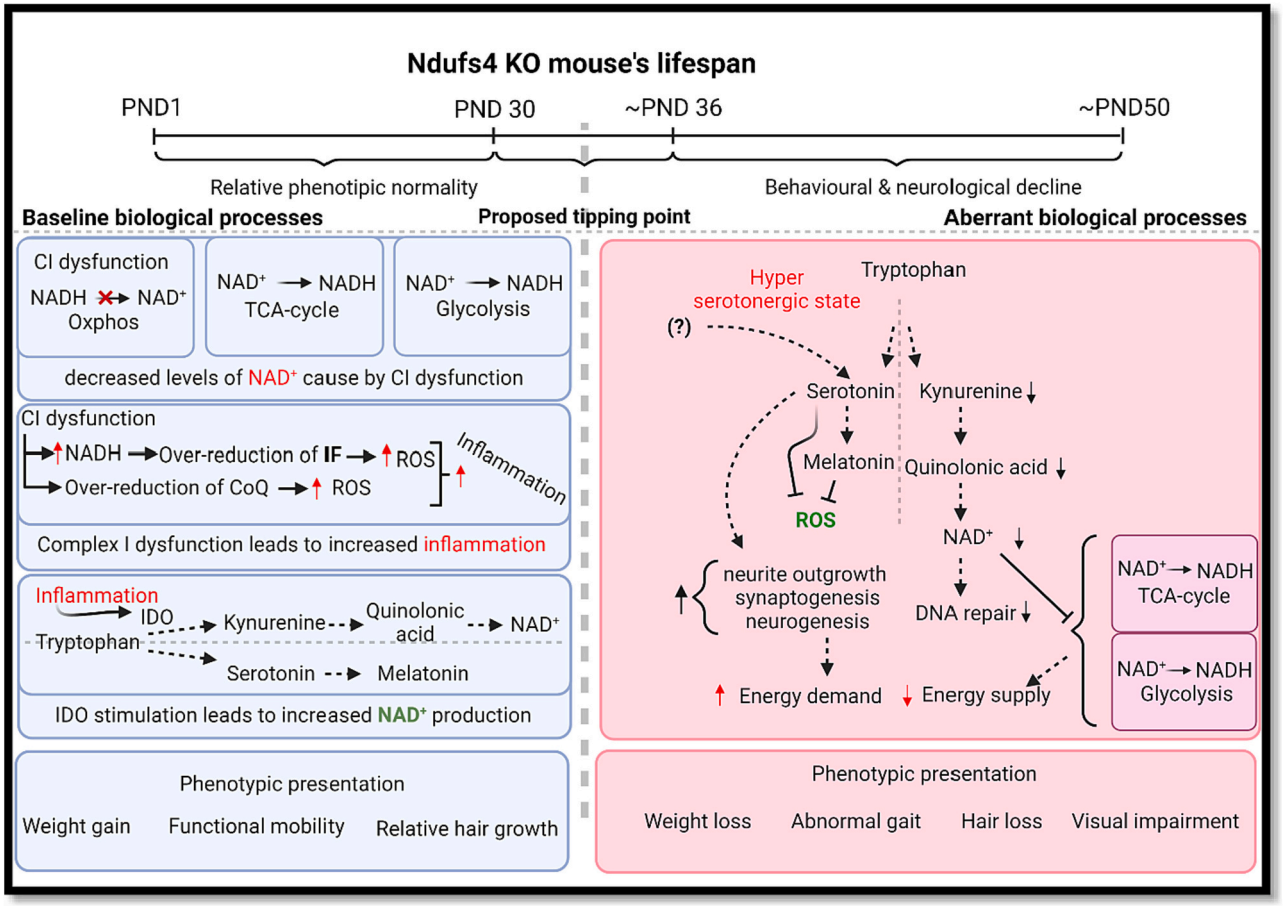

Fig. 8. Phenotypical and biological destabilization due to mitochondrial dysfunction
The data in the current study suggests that a mechanism involving the tryptophan metabolic pathway, preceding their early death, may be involved in the aberrant biological functions observed in the Ndufs4 mice. The tricarboxylic acid cycle and glycolysis are the two energy producing processes that compensate for the lack of ATP production caused by complex I dysfunction. The consequent decrease in NAD^+ and increase in ROS could lead to increased activation of inflammatory markers, which in turn would upregulate kynurenine synthesis to compensate for the decrease in NAD^+. Conversely, at the so-called tipping point, the hyper serotonergic state would steer tryptophan turnover away from kynurenine and further deplete NAD^+. This is noteworthy, as NAD^+ precursor supplementation inhibits neuron excitability and lengthens the lifespan of the Ndufs4 KO mice, thereby supporting the narrative that hyperserotonergia could signal the "tipping point" of the KO life cycle. Ultimately, this would lead to a decreased energy supply at a point of the mouse's life characterized by neural development and an overall increased energy demand. ATP: adenosine triphosphate; CoQ: cytochrome *c* reductase; CI: complex 1; IDO: indoleamine 2,3-dioxygenase; IF: NADH oxidase site; PND: postnatal day; NAD^+: nicotinamide adenine dinucleotide; ROS: reactive oxygen species. Created with BioRender.com.

phenotype may represent an obstacle in comprehensively validating the *Ndufs4* KO model for major depressive disorder, even though the behavioural alterations displayed by the *Ndufs4* KO mouse does strengthen the neuropsychiatric similarities that parallel mitochondrial diseases, especially comorbid depression and psychosis (Anglin et al., 2012). Pharmacological interventions to assess predictive validation, which would require investigational periods longer than the PND 28–35 window, may also be challenging.

Kato et al. (2018) found an association between lowered impulsivity behaviour and mitochondrial dysfunction with behaviour akin to bipolar disorder. Similarly, Valvassori et al. (2019) also observed a relatively quick shift (7 days) between manic and depressive-like behaviour in the ouabain model of bipolar disorder. Regardless, that these juvenile KO mice are at an age associated with energy demanding neurodevelopmental processes, could explain such a drastic behavioural change. At PND35, the mice are close to an age (PND40) where their overall health rapidly declines due to compromised mitochondrial function (Kruse et al., 2008), which could then contribute to aberrant brain function. In fact, brain maturation might compound the effects of mitochondrial dysfunction in this model (2008). Building on this hypothesis, Fig. 8 summarizes such a developmental shift in bio-energetic homeostasis. Based on the current findings, a tipping point is suggested to separate the relative normal phenotype from the observed behavioural and neurological decline. Here, the baseline biological processes of the *Ndufs4* KO mouse, shifts to a more detrimental or aberrant state – which in turn highlights the value of further investigating the HET *Ndufs4* genotype as a viable substitute.

In terms of brain neurochemical changes, mitochondrial dysfunction, oxidative stress, and neuro-inflammation have been associated with depressive symptoms, such as suicidal ideation and attempts (Liu et al., 2015; Vasupanrajit et al., 2022). Reduced glutathione (GSH) is a vital intra- and extracellular antioxidant, which is converted to its oxidized form, i.e., GSSG, under conditions of oxidative stress (Zitka et al., 2012). The molar GSH/GSSG ratio is therefore a valuable biomarker to determine cellular redox state (Enns and Cowan, 2017). That *Ndufs4* KO mice had significantly higher striatal and hippocampal GSH/GSSG values, compared to the HET and WT counterparts (Fig. 5), suggest a redox dysregulation. Of note, HET strongly trended to differ from WT in terms of redox state, underlining at least a neurochemical genotype difference to be explored in prospective studies. Still, the increased GSH/GSSG ratio of the KO mice is noteworthy, as the inherent dysfunctional complex I of the KO mouse causes ubiquinone (also known as co-enzyme Q10; CoQ) to become over reduced via electrons from complex II, which in turn increases ROS production (Scialò et al., 2017). However, that complex I dysfunction also inhibits the conversion of NADH to NAD^+ (Lee et al., 2019), might explain the greater redox dysregulation (see Fig. 8). Indeed, decreased (Miller et al., 2021) and unaltered (Kayser et al., 2016) oxidized proteins in *Ndufs4* KO mice support our findings. Supporting the redox state (GSH/GSSG) findings, serotonin has strong antioxidant properties (Sarikaya and Gulcin, 2013), and was higher in the cortex and hippocampus of the *Ndufs4* KO mice, compared to HET controls (Figs. 6A and B) on PND36. That serotonin levels were increased in KO mice is noteworthy as brain samples were collected <24 h after these animals displayed decreased immobility in the forced swim test and may therefore explain the normalization of depressive-like behaviour (Fig. 3), risk resilience observed in the mirror box test (Fig. 4A), and the lack of oxidative stress.

The above changes occurred despite the theoretical increase in reactive oxygen species production caused by mitochondrial complex I dysfunction. To this point, Kato et al. (2018) reported that adenine nucleotide translocator-1 (ANT1) heterozygous mice (used to study mitochondrial dysfunction in bipolar disorder) also present with a "hyperserotonergic state". This hyperserotonergic state increases intramitochondrial calcium and hyperphosphorylation of inositol 1,4,5-trisphosphate receptor type 1 (Martin-Perez et al., 2020) to increase intramitochondrial calcium levels and thus alter neuron excitability (see Fig. 8). Ouabain also increases neuron excitability and impairs the calcium depuration rate (Martin, 1966; McCarren and Alger, 1987) to induce manic-like states in rodents. Calcium dysregulation induced NAD^+ redox imbalance (Lee et al., 2016) may explain why NAD^+ precursor supplementation increases the lifespan of *Ndufs4* KO mice (Lee et al., 2019) by attenuating redox imbalance, and inhibiting neuron over excitability. The potential neurochemical similarities between the ANT1, ouabain and *Ndufs4* KO mice are especially notable, as the ouabain model is a widely accepted model for bipolar disorder (Valvassori et al., 2019), with the ANT1 also showing promise in this regard (van Rensburg et al., 2022). Because decreased mitochondrial complex I activity is observed in bipolar patients (Andreazza et al., 2010), these animal models could aid in improving our current understanding of this condition. Furthermore, hyperserotonergia observed on PND36 may contribute to the drastic decline in overall health, behaviour, and neurological symptoms evident from PND36 onwards (Johnson et al., 2020; Kruse et al., 2008), especially by disrupting brain development Esaki et al. (2005)), and further supporting the neurological symptoms typically displayed by KO mice after PND40 (refer to Fig. 8).

NAD^+ redox dysregulation is known to reside within KO mice (Lee et al., 2019). A close interrelationship resides between tryptophan and kynurenine and serotonin synthesis, with tryptophan hydroxylase and indoleamine 2,3-dioxygenase (IDO) mediating serotonin and kynurenine synthesis respectively (Correia and Vale, 2022) (Fig. 8). Increased serotonin may hamper NAD^+ production (see Fig. 8) (Miura et al., 2008), resulting in the above-noted altered redox state. Indeed, *Ndufs4* KO mice had significantly increased hippocampal and cortical serotonin/tryptophan levels, compared only to the HET controls (Fig. 6). KO mice also had increased cortical kynurenine/tryptophan turnover (Fig. 6), suggesting increased kynurenine synthesis and a selective shift towards enhanced serotonin versus kynurenine synthesis. The increased inflammation previously reported in the KO mice (Liu et al., 2015; Miller et al., 2021) could underlie such an inflammatory-induced stimulation of IDO (Maes, 2011), partly explaining the increased kynurenine levels observed here and the development of a hyperserotonergic state noted earlier. Decreased kynurenic acid/kynurenine ratio (Fig. 6) might also hint towards increased quinolinic acid (opposed to kynurenic acid) to produce NAD^+, although warrants further exploration. As reviewed by Marx et al. (2021), major depressive disorder and bipolar depression present with decreased levels of tryptophan and kynurenine and kynurenic acid/kynurenine, and increased kynurenine/tryptophan ratios, all of which are in contrast to that measured in the *Ndufs4* KO mice. That said, our findings may specifically represent a "high risk" presyndromic state that underlies species-specific neurodevelopmental changes as a function of illness severity over time.

Certain limitations of the current study must however be noted. Firstly, while the bio-behavioural profile of the *Ndufs4* KO mice is promising in terms of mood-related disorders, a longitudinal study will reveal deeper underpinnings of the neurological and behavioural shifts of the Ndufs4 mouse, which in turn might refine our understanding of the mechanistic domain. Moreover, the limited lifespan of the KO mice is an obvious obstacle, stressing the potential of performing subsequent work in the HET genotype. Also, despite locomotor adjusted depressive-like behaviours, the influence of decreased locomotor activity on these behaviours should be more closely scrutinized. Finally, future studies should include an appropriate pharmacological intervention to expand on the underlying biology of the model, as well as its predictive validity.

Taken together, the *Ndufs4* KO mice potentially presents with risk resilience and transient depressive-like behaviour between PND30 and 35, which is coupled with a hyperserotonergic state and specific redox-inflammatory changes related to the glutathione and tryptophan-kynurenine pathways. Based on these findings, our results allow us to reject the null hypothesis and conclude that because these alterations are thought to be caused by the mitochondrial dysfunctional construct of these animals, the *Ndufs4* KO mouse may be a useful model to further investigate the mechanisms of mood-related conditions in patients with

mitochondrial diseases, even Leigh syndrome. Additionally, considering the differences in neurochemical profile between the HET and WT genotypes (specifically following a battery of behavioural tests), the *Ndufs4* HET may be a more viable alternative to investigate the bioenergetic construct of mood disorders.

Funding

BHH is supported by the SAMRC Unit on Risk & Resilience in Mental Disorders.

Compliance with ethical standards

All experimental procedures were approved by the NWU-AnimCare research ethics committee (approval number: NWU-00420-21-A5) and complied with the South African National Standard (SANS) for the Care and Use of Animals for Scientific Purposes (SANS 10386:2008), which all align with the ARRIVE guidelines (Du Sert et al., 2020).

CRediT authorship contribution statement

Daniël J. van Rensburg: Formal analysis, Investigation, Methodology, Visualization, Writing – original draft, Writing – review & editing. **Zander Lindeque:** Conceptualization, Resources, Supervision, Writing – original draft, Writing – review & editing. **Brian H. Harvey:** Funding acquisition, Writing – original draft, Writing – review & editing. **Stephan F. Steyn:** Conceptualization, Formal analysis, Project administration, Supervision, Visualization, Writing – original draft, Writing – review & editing.

Declaration of competing interest

None to declare.

Data availability

Data will be made available on request.

Acknowledgements

The authors would like to acknowledge and thank Dr. Francois Viljoen for his assistance with neurochemical analyses. And Mr. Cor Bester, Mrs. Antoinette Fick, Mr. Kobus Venter and Sr Irene Serage for their support and assistance in overseeing the welfare of the animals. This work emanated from a Masters (MSc) degree at the NWU (DJvR).

Appendix A. Supplementary data

Supplementary data to this article can be found online at https://doi.org/10.1016/j.pbb.2023.173689.

References

Allen, J., Romay-Tallon, R., Brymer, K.J., Caruncho, H.J., Kalynchuk, L.E., 2018. Mitochondria and mood: mitochondrial dysfunction as a key player in the manifestation of depression. Front. Neurosci. 12, 386.
Andreazza, A.C., Shao, L., Wang, J.-F., Young, L.T., 2010. Mitochondrial complex I activity and oxidative damage to mitochondrial proteins in the prefrontal cortex of patients with bipolar disorder. Arch. Gen. Psychiatry 67 (4), 360.
Anglin, R.E., Garside, S.L., Tarnopolsky, M.A., Mazurek, M.F., Rosebush, P.I., 2012. The psychiatric manifestations of mitochondrial disorders: a case and review of the literature. J. Clin. Psychiatry 73 (4), 15930.
Avetisyan, A., Samokhin, A., Alexandrova, I., Zinovkin, R., Simonyan, R., Bobkova, N., 2016. Mitochondrial dysfunction in neocortex and hippocampus of olfactory bulbectomized mice, a model of Alzheimer's disease. Biochem. Mosc. 81 (6), 615–623.
Balakrishnan, R., Vijayraja, D., Mohankumar, T., Manimaran, D., Ganesan, P., Choi, D.-K., Elangovan, N., 2021. Isolongifolene mitigates rotenone-induced dopamine depletion and motor deficits through anti-oxidative and anti-apoptotic effects in a rat model of Parkinson's disease. J. Chem. Neuroanat. 112, 101890.
Benzi, G., Moretti, A., 1995. Age-and peroxidative stress-related modifications of the cerebral enzymatic activities linked to mitochondria and the glutathione system. Free Radic. Biol. Med. 19 (1), 77–101.
Bjørklund, G., Peana, M., Maes, M., Dadar, M., Severin, B., 2021. The glutathione system in Parkinson's disease and its progression. Neurosci. Biobehav. Rev. 120, 470–478.
Bleys, D., Luyten, P., Soenens, B., Claes, S., 2018. Gene-environment interactions between stress and 5-HTTLPR in depression: a meta-analytic update. J. Affect. Disord. 226, 339–345.
Boeschoten, R.E., Braamse, A.M., Beekman, A.T., Cuijpers, P., van Oppen, P., Dekker, J., Uitdehaag, B.M., 2017. Prevalence of depression and anxiety in multiple sclerosis: a systematic review and meta-analysis. J. Neurol. Sci. 372, 331–341.
Breuer, M.E., Willems, P.H.G.M., Russel, F.G.M., Koopman, W.J.H., Smeitink, J.A.M., 2012. Modeling mitochondrial dysfunctions in the brain: from mice to men. J. Inherit. Metab. Dis. 35 (2), 193–210.
Bustamante, J., Czerniczyniec, A., Lores-Arnaiz, S., 2007. Brain nitric oxide synthases and mitochondrial function. Front. Biosci. 12 (3), 1034–1040.
Calvaruso, M.A., Willems, P., van den Brand, M., Valsecchi, F., Kruse, S., Palmiter, R., Smeitink, J., Nijtmans, L., 2012. Mitochondrial complex III stabilizes complex I in the absence of NDUFS4 to provide partial activity. Hum. Mol. Genet. 21 (1), 115–120.
Carola, V., D'Olimpio, F., Brunamonti, E., Mangia, F., Renzi, P., 2002. Evaluation of the elevated plus-maze and open-field tests for the assessment of anxiety-related behaviour in inbred mice. Behav. Brain Res. 134 (1–2), 49–57.
Castagné, V., Moser, P., Roux, S., Porsolt, R.D., 2011. Rodent models of depression: forced swim and tail suspension behavioral despair tests in rats and mice. Curr. Protoc. Neurosci. 55 (1) (8.10 A. 11-18.10 A. 14).
Chen, F., Wegener, G., Madsen, T.M., Nyengaard, J.R., 2013. Mitochondrial plasticity of the hippocampus in a genetic rat model of depression after antidepressant treatment. Synapse 67 (3), 127–134.
Chen, Y., McMillan-Ward, E., Kong, J., Israels, S.J., Gibson, S.B., 2007. Mitochondrial electron-transport-chain inhibitors of complexes I and II induce autophagic cell death mediated by reactive oxygen species. J. Cell Sci. 120 (23), 4155–4166.
Cohen, J., 2013. Statistical Power Analysis for the Behavioral Sciences. Academic Press.
Correia, A.S., Vale, N., 2022. Tryptophan metabolism in depression: a narrative review with a focus on serotonin and kynurenine pathways. Int. J. Mol. Sci. 23 (15), 8493.
Crawley, J., Goodwin, F.K., 1980. Preliminary report of a simple animal behavior model for the anxiolytic effects of benzodiazepines. Pharmacol. Biochem. Behav. 13 (2), 167–170.
Cryan, J.F., Markou, A., Lucki, I., 2002. Assessing antidepressant activity in rodents: recent developments and future needs. Trends Pharmacol. Sci. 23 (5), 238–245.
Cryan, J.F., Mombereau, C., Vassout, A., 2005. The tail suspension test as a model for assessing antidepressant activity: review of pharmacological and genetic studies in mice. Neurosci. Biobehav. Rev. 29 (4–5), 571–625.
Cumming, G., 2014. The new statistics: why and how. Psychol. Sci. 25 (1), 7–29.
Damri, O., Asslih, S., Shemesh, N., Natour, S., Noori, O., Daraushe, A., Einat, H., Kara, N., Las, G., Agam, G., 2021. Using mitochondrial respiration inhibitors to design a novel model of bipolar disorder-like phenotype with construct, face and predictive validity. Transl. Psychiatry 11 (1), 1–14.
Du Sert, N.P., Ahluwalia, A., Alam, S., Avey, M.T., Baker, M., Browne, W.J., Clark, A., Cuthill, I.C., Dirnagl, U., Emerson, M., 2020. Reporting animal research: explanation and elaboration for the ARRIVE guidelines 2.0. PLoS Biol. 18 (7), e3000411.
Ellis, P.D., 2010. The Essential Guide to Effect Sizes: Statistical Power, Meta-analysis, and the Interpretation of Research Results. Cambridge University Press.
Emmerzaal, T.L., Jacobs, L., Geenen, B., Verweij, V., Morava, E., Rodenburg, R.J., Kozicz, T., 2020a. Chronic fluoxetine or ketamine treatment differentially affects brain energy homeostasis which is not exacerbated in mice with trait suboptimal mitochondrial function. Eur. J. Neurosci. 53 (9), 2986–3001.
Emmerzaal, T.L., Preston, G., Geenen, B., Verweij, V., Wiesmann, M., Vasileiou, E., Grüter, F., de Groot, C., Schoorl, J., de Veer, R., 2020b. Impaired mitochondrial complex I function as a candidate driver in the biological stress response and a concomitant stress-induced brain metabolic reprogramming in male mice. Transl. Psychiatry 10 (1), 1–13.
Enns, G.M., Cowan, T.M., 2017. Glutathione as a redox biomarker in mitochondrial disease—implications for therapy. J. Clin. Med. 6 (5), 50.
Esaki, T., Cook, M., Shimoji, K., Murphy, D.L., Sokoloff, L., Holmes, A., 2005. Developmental disruption of serotonin transporter function impairs cerebral responses to whisker stimulation in mice. Proc. Natl. Acad. Sci. 102 (15), 5582–5587.
Fattal, O., Link, J., Quinn, K., Cohen, B.H., Franco, K., 2007. Psychiatric comorbidity in 36 adults with mitochondrial cytopathies. CNS Spectr. 12 (6), 429–438.
Fuss, J., Richter, S.H., Steinle, J., Deubert, G., Hellweg, R., Gass, P., 2013. Are you real? Visual simulation of social housing by mirror image stimulation in single housed mice. Behav. Brain Res. 243, 191–198.
Gorton, L.M., Vuckovic, M.G., Vertelkina, N., Petzinger, G.M., Jakowec, M.W., Wood, R. I., 2010. Exercise effects on motor and affective behavior and catecholamine neurochemistry in the MPTP-lesioned mouse. Behav. Brain Res. 213 (2), 253–262.
Grace, J., Chandrasekaran, K., Morgan, W., 2006. Mitochondrial dysfunction, persistently elevated levels of reactive oxygen species and radiation-induced genomic instability: a review. Mutagenesis 21 (6), 361–367.
Hu, Q., Uversky, V.N., Huang, M., Kang, H., Xu, F., Liu, X., Lian, L., Liang, Q., Jiang, H., Liu, A., Zhang, C., Pan-Montojo, F., Zhu, S., 2016. Baicalein inhibits α-synuclein oligomer formation and prevents progression of α-synuclein accumulation in a rotenone mouse model of Parkinson's disease. Biochim. Biophys. Acta (BBA) - Mol. Basis Dis. 1862 (10), 1883–1890.
Johnson, S.C., Kayser, E.-B., Bornstein, R., Stokes, J., Bitto, A., Park, K.Y., Pan, A., Sun, G., Raftery, D., Kaeberlein, M., 2020. Regional metabolic signatures in the

ndufs4 (KO) mouse brain implicate defective glutamate/α-ketoglutarate metabolism in mitochondrial disease. Mol. Genet. Metab. 130 (2), 118–132.
Kara, N.Z., Einat, H., 2013. Rodent models for mania: practical approaches. Cell Tissue Res. 354 (1), 191–201.
Kato, T.M., Kubota-Sakashita, M., Fujimori-Tonou, N., Saitow, F., Fuke, S., Masuda, A., Itohara, S., Suzuki, H., Kato, T., 2018. ANT1 mutant mice bridge the mitochondrial and serotonergic dysfunctions in bipolar disorder. Mol. Psychiatry 23 (10), 2039–2049.
Kayser, E.-B., Sedensky, M.M., Morgan, P.G., 2016. Region-specific defects of respiratory capacities in the Ndufs4(KO) mouse brain. PLoS One 11 (1), e0148219.
Keller, R., Oke, A., Mefford, I., Adams, R.N., 1976. Liquid chromatographic analysis of catecholamines routine assay for regional brain mapping. Life Sci. 19 (7), 995–1003.
Kliethermes, C.L., Finn, D.A., Crabbe, J.C., 2003. Validation of a modified mirrored chamber sensitive to anxiolytics and anxiogenics in mice. Psychopharmacology 169 (2), 190–197.
Kruse, S.E., Watt, W.C., Marcinek, D.J., Kapur, R.P., Schenkman, K.A., Palmiter, R.D., 2008. Mice with mitochondrial complex I deficiency develop a fatal encephalomyopathy. Cell Metab. 7 (4), 312–320.
Lakens, D., 2013. Calculating and reporting effect sizes to facilitate cumulative science: a practical primer for t-tests and ANOVAs. Front. Psychol. 4, 863.
Lee, C.F., Chavez, J.D., Garcia-Menendez, L., Choi, Y., Roe, N.D., Chiao, Y.A., Edgar, J.S., Goo, Y.A., Goodlett, D.R., Bruce, J.E., Tian, R., 2016. Normalization of nad$^+$ redox balance as a therapy for heart failure. Circulation 134 (12), 883–894.
Lee, C.F., Caudal, A., Abell, L., Nagana Gowda, G.A., Tian, R., 2019. Targeting NAD+ metabolism as interventions for mitochondrial disease. Sci. Rep. 9 (1).
LeMoult, J., Humphreys, K.L., Tracy, A., Hoffmeister, J.-A., Ip, E., Gotlib, I.H., 2020. Meta-analysis: exposure to early life stress and risk for depression in childhood and adolescence. J. Am. Acad. Child Adolesc. Psychiatry 59 (7), 842–855.
Lindeque, J.Z., Matthyser, A., Mason, S., Louw, R., Taute, C.J.F., 2018. Metabolomics reveals the depletion of intracellular metabolites in HepG2 cells after treatment with gold nanoparticles. Nanotoxicology 12 (3), 251–262.
Liu, L., Zhang, K., Sandoval, H., Yamamoto, S., Jaiswal, M., Sanz, E., Li, Z., Hui, J., Graham, B.H., Quintana, A., 2015. Glial lipid droplets and ros induced by mitochondrial defects promote neurodegeneration. Cell 160 (1–2), 177–190.
Maes, M., 2011. Depression is an inflammatory disease, but cell-mediated immune activation is the key component of depression. Prog. Neuro-Psychopharmacol. Biol. Psychiatry 35 (3), 664–675.
Manji, H., Kato, T., Di Prospero, N.A., Ness, S., Beal, M.F., Krams, M., Chen, G., 2012. Impaired mitochondrial function in psychiatric disorders. Nat. Rev. Neurosci. 13 (5), 293–307.
Martin, A., 1966. Quantal nature of synaptic transmission. Physiol. Rev. 46 (1), 51–66.
Martin-Perez, M., Grillo, A.S., Ito, T.K., Valente, A.S., Han, J., Entwisle, S.W., Huang, H. Z., Kim, D., Yajima, M., Kaeberlein, M., 2020. PKC downregulation upon rapamycin treatment attenuates mitochondrial disease. Nat. Metab. 2 (12), 1472–1481.
Marx, W., McGuinness, A.J., Rocks, T., Ruusunen, A., Cleminson, J., Walker, A.J., Gomes-da-Costa, S., Lane, M., Sanches, M., Diaz, A.P., 2021. The kynurenine pathway in major depressive disorder, bipolar disorder, and schizophrenia: a meta-analysis of 101 studies. Mol. Psychiatry 26 (8), 4158–4178.
McCarren, M., Alger, B.E., 1987. Sodium-potassium pump inhibitors increase neuronal excitability in the rat hippocampal slice: role of a Ca2+−dependent conductance. J. Neurophysiol. 57 (2), 496–509.
Miller, H.C., Louw, R., Mereis, M., Venter, G., Boshoff, J.-D., Mienie, L., Van Reenen, M., Venter, M., Lindeque, J.Z., Domínguez-Martínez, A., Quintana, A., Van Der Westhuizen, F.H., 2021. Metallothionein 1 overexpression does not protect against mitochondrial disease pathology in ndufs4 knockout mice. Mol. Neurobiol. 58 (1), 243–262.
Missiroli, S., Genovese, I., Perrone, M., Vezzani, B., Vitto, V.A.M., Giorgi, C., 2020. The role of mitochondria in inflammation: from cancer to neurodegenerative disorders. J. Clin. Med. 9 (3), 740.
Miura, H., Ozaki, N., Sawada, M., Isobe, K., Ohta, T., Nagatsu, T., 2008. A link between stress and depression: shifts in the balance between the kynurenine and serotonin pathways of tryptophan metabolism and the etiology and pathophysiology of depression. Stress 11 (3), 198–209.
Mncube, K., Harvey, B.H., 2022. Bio-behavioural changes in treatment-resistant socially isolated FSL rats show variable or improved response to combined fluoxetine-olanzapine versus olanzapine treatment. IBRO Neurosci. Rep. 13, 284–298.
Morava, E., Gardeitchik, T., Kozicz, T., De Boer, L., Koene, S., De Vries, M., McFarland, R., Roobol, T., Rodenburg, R., Verhaak, C., 2010. Depressive behaviour in children diagnosed with a mitochondrial disorder. Mitochondrion 10 (5), 528–533.
Murphy, M.P., 2018. Newly made mitochondrial dna drives inflammation. Nature 560 (7717), 176–177.
Okano, M., Takahata, K., Sugimoto, J., Muraoka, S., 2019. Selegiline recovers synaptic plasticity in the medial prefrontal cortex and improves corresponding depression-like behavior in a mouse model of Parkinson's disease. Front. Behav. Neurosci. 13, 176.
Pan-Montojo, F., Anichtchik, O., Dening, Y., Knells, L., Pursche, S., Jung, R., Jackson, S., Gille, G., Spillantini, M.G., Reichmann, H., Funk, R., 2010. Progression of Parkinson's disease pathology is reproduced by intragastric administration of rotenone in mice. Nat. Prec. 1-1.
Patten, S.B., Marrie, R.A., Carta, M.G., 2017. Depression in multiple sclerosis. Int. Rev. Psychiatry 29 (5), 463–472.
Pich, E.M., Samanin, R., 1989. A two-compartment exploratory model to study anxiolytic/anxiogenic effects of drugs in the rat. Pharmacol. Res. 21 (5), 595–602.
Przedborski, S., Jackson-Lewis, V., Djaldetti, R., Liberatore, G., Vila, M., Vukosavic, S., Almer, G., 2000. The parkinsonian toxin mptp: action and mechanism. Restor. Neurol. Neurosci. 16 (2), 135–142.
Reddy, P.H., Reddy, T.P., Manczak, M., Calkins, M.J., Shirendeb, U., Mao, P., 2011. Dynamin-related protein 1 and mitochondrial fragmentation in neurodegenerative diseases. Brain Res. Rev. 67 (1–2), 103–118.
Regenass, W., Möller, M., Harvey, B.H., 2018. Studies into the anxiolytic actions of agomelatine in social isolation reared rats: role of corticosterone and sex. J. Psychopharmacol. 32 (2), 134–145.
van Rensburg, D.J., Lindeque, J.Z., Harvey, B.H., Steyn, S.F., 2022. Reviewing the mitochondrial dysfunction paradigm in rodent models as platforms for neuropsychiatric disease research. Mitochondrion 64, 82–102.
Rezin, G.T., Amboni, G., Zugno, A.I., Quevedo, J., Streck, E.L., 2009. Mitochondrial dysfunction and psychiatric disorders. Neurochem. Res. 34 (6), 1021–1029.
Salim, S., 2014. Oxidative stress and psychological disorders. Curr. Neuropharmacol. 12 (2), 140–147.
Santiago, R.M., Barbieiro, J., Lima, M.M., Dombrowski, P.A., Andreatini, R., Vital, M.A., 2010. Depressive-like behaviors alterations induced by intranigral mptp, 6-ohda, lps and rotenone models of Parkinson's disease are predominantly associated with serotonin and dopamine. Prog. Neuro-Psychopharmacol. Biol. Psychiatry 34 (6), 1104–1114.
Sarikaya, S., Gulcin, I., 2013. Radical scavenging and antioxidant capacity of serotonin. Curr. Bioact. Compd. 9 (2), 143–152.
Scialò, F., Fernández-Ayala, D.J., Sanz, A., 2017. Role of mitochondrial reverse electron transport in ROS signaling: potential roles in health and disease. Front. Physiol. 8, 428.
Seewoo, B.J., Hennessy, L.A., Feindel, K.W., Etherington, S.J., Croarkin, P.E., Rodger, J., 2020. Validation of chronic restraint stress model in young adult rats for the study of depression using longitudinal multimodal MR imaging. eNeuro 7 (4).
Seibenhener, M.L., Wooten, M.C., 2015. Use of the open field maze to measure locomotor and anxiety-like behavior in mice. J. Vis. Exp. 96.
Sharma, N., Jamwal, S., Kumar, P., 2016. Beneficial effect of antidepressants against rotenone induced Parkinsonism like symptoms in rats. Pathophysiology 23 (2), 123–134.
Sharma, S., Akundi, R.S., 2019. Mitochondria: a connecting link in the major depressive disorder jigsaw. Curr. Neuropharmacol. 17 (6), 550–562.
Smaga, I., Niedzielska, E., Gawlik, M., Moniczewski, A., Krzek, J., Przegaliński, E., Pera, J., Filip, M., 2015. Oxidative stress as an etiological factor and a potential treatment target of psychiatric disorders. Part 2. Depression, anxiety, schizophrenia and autism. Pharmacol. Rep. 67 (3), 569–580.
Smythe, J.W., Murphy, D., Bhatnagar, S., Timothy, C., Costall, B., 1996. Muscarinic antagonists are anxiogenic in rats tested in the black-white box. Pharmacol. Biochem. Behav. 54 (1), 57–63.
Soares-Cunha, C., Coimbra, B., Borges, S., Domingues, A.V., Silva, D., Sousa, N., Rodrigues, A.J., 2018. Mild prenatal stress causes emotional and brain structural modifications in rats of both sexes. Front. Behav. Neurosci. 12, 129.
Solaro, C., Gamberini, G., Masuccio, F.G., 2018. Depression in multiple sclerosis: epidemiology, aetiology, diagnosis and treatment. CNS Drugs 32 (2), 117–133.
Stenton, S.L., Zou, Y., Cheng, H., Liu, Z., Wang, J., Shen, D., Jin, H., Ding, C., Tang, X., Sun, S., Han, H., Ma, Y., Zhang, W., Jin, R., Wang, H., Sun, D., Lv, J.L., Prokisch, H., Fang, F., 2022. Leigh syndrome: a study of 209 patients at the Beijing children's hospital. Ann. Neurol. 91 (4), 466–482.
Steyn, S.F., Harvey, B.H., Brink, C.B., 2020. Pre-pubertal, low-intensity exercise does not require concomitant venlafaxine to induce robust, late-life antidepressant effects in Flinders sensitive line rats. Eur. J. Neurosci. 52 (8), 3979–3994.
Sullivan, G.M., Feinn, R., 2012. Using effect size - or why the *p* value is not enough. J. Grad. Med. Educ. 4 (3), 279–282.
Swanepoel, T., Möller, M., Harvey, B.H., 2018. N-acetyl cysteine reverses bio-behavioural changes induced by prenatal inflammation, adolescent methamphetamine exposure and combined challenges. Psychopharmacology 235 (1), 351–368.
Swathi, G., Bhuvaneswar, C., Rajendra, W., 2013. Alterations of cholinergic neurotransmission in rotenone induced parkinson's disease: protective role of bacopa monnieri. Int. J. Pharm. Bio Sci. 3, 286–292.
Terburgh, K., Lindeque, Z., Mason, S., Van der Westhuizen, F., Louw, R., 2019. Metabolomics of Ndufs4−/− skeletal muscle: adaptive mechanisms converge at the ubiquinone-cycle. Biochim. Biophys. Acta (BBA) - Mol. Basis Dis. 1865 (1), 98–106.
Valvassori, S.S., Dal-Pont, G.C., Resende, W.R., Varela, R.B., Lopes-Borges, J., Cararo, J. H., Quevedo, J., 2019. Validation of the animal model of bipolar disorder induced by ouabain: face, construct and predictive perspectives. Transl. Psychiatry 9 (1), 1–11.
Van De Wal, M.A.E., Adjobo-Hermans, M.J.W., Keijer, J., Schirris, T.J.J., Homberg, J.R., Wieckowski, M.R., Grefte, S., Van Schothorst, E.M., Van Karnebeek, C., Quintana, A., Koopman, W.J.H., 2022. Ndufs4 knockout mouse models of Leigh syndrome: pathophysiology and intervention. Brain 145 (1), 45–63.
Varga, T.G., De Toledo Simões, J.G., Siena, A., Henrique, E., Da Silva, R.C.B., Dos Santos Bioni, V., Ramos, A.C., Rosenstock, T.R., 2021. Haloperidol rescues the schizophrenia-like phenotype in adulthood after rotenone administration in neonatal rats. Psychopharmacology 238, 2569–2585.
Vasupanrajit, A., Jirakran, K., Tunvirachaisakul, C., Solmi, M., Maes, M., 2022. Inflammation and nitro-oxidative stress in current suicidal attempts and current suicidal ideation: a systematic review and meta-analysis. Mol. Psychiatry 27 (3), 1350–1361.
Vogel, R.O., van den Brand, M.A., Rodenburg, R.J., van den Heuvel, L.P., Tsuneoka, M., Smeitink, J.A., Nijtmans, L.G., 2007. Investigation of the complex I assembly chaperones B17. 2L and ndufaF1 in a cohort of CI deficient patients. Mol. Genet. Metab. 91 (2), 176–182.

Wajner, M., Amaral, A.U., 2016. Mitochondrial dysfunction in fatty acid oxidation disorders: insights from human and animal studies. Biosci. Rep. 36 (1).
Walf, A.A., Koonce, C., Manley, K., Frye, C.A., 2009. Proestrous compared to diestrous wildtype, but not estrogen receptor beta knockout, mice have better performance in the spontaneous alternation and object recognition tasks and reduced anxiety-like behavior in the elevated plus and mirror maze. Behav. Brain Res. 196 (2), 254–260.
Wallace, K.B., 2007. Adriamycin-induced interference with cardiac mitochondrial calcium homeostasis. Cardiovasc. Toxicol. 7 (2), 101–107.
Wang, D., Levine, J.L., Avila-Quintero, V., Bloch, M., Kaffman, A., 2020. Systematic review and meta-analysis: effects of maternal separation on anxiety-like behavior in rodents. Transl. Psychiatry 10 (1), 1–12.
Wang, Y., Xu, E., Musich, P.R., Lin, F., 2019. Mitochondrial dysfunction in neurodegenerative diseases and the potential countermeasure. CNS Neurosci. Ther. 25 (7), 816–824.
Wen, L., Jin, Y., Li, L., Sun, S., Cheng, S., Zhang, S., Zhang, Y., Svenningsson, P., 2014. Exercise prevents raphe nucleus mitochondrial overactivity in a rat depression model. Physiol. Behav. 132, 57–65.
Wolmarans, D.W., Prinsloo, M., Seedat, S., Stein, D.J., Harvey, B.H., de Brouwer, G., 2022. Escitalopram and lorazepam differentially affect nesting and open field behaviour in deer mice exposed to an anxiogenic environment. Neurosci. Res. 177, 85–93.
von Wrangel, C., Schwabe, K., John, N., Krauss, J.K., Alam, M., 2015. The rotenone-induced rat model of Parkinson's disease: behavioral and electrophysiological findings. Behav. Brain Res. 279, 52–61.
Zhao, R.Z., Jiang, S., Zhang, L., Yu, Z.B., 2019. Mitochondrial electron transport chain, ROS generation and uncoupling. Int. J. Mol. Med. 44 (1), 3–15.
Zitka, O., Skalickova, S., Gumulec, J., Masarik, M., Adam, V., Hubalek, J., Trnkova, L., Kruseova, J., Eckschlager, T., Kizek, R., 2012. Redox status expressed as GSH: GSSG ratio as a marker for oxidative stress in paediatric tumour patients. Oncol. Lett. 4 (6), 1247–1253.